Optical image recognition using photorefractive crystal plates

M. L. Hsieh, S. H. Lin, K. Y. Hsu, and T. C. Hsieh[*]

Institute of Electro-Optical Engineering
[*]Department of Electro-Physics
National Chiao Tung university
Hsinchu, Taiwan, R. O. C.

and
S. P. Lin, T. S. Yeh, L. J. Hu, S. L. Tu, and H. Chang
Materials Research and Development Center
Chung Shan Institute of Science and Technology
Lung-Tan, Taiwan, R. O. C.

Abstract

We demonstrate a real-time optical image recognition system using photorefractive thin plates. The effects of donor/acceptor concentration ratio in thin lithium niobate crystal plates on the photorefractive response time and the grating diffraction efficiency are presented.

Keywords: Optical image recognition, Optical neural networks, Photorefractive crystals.

1. Introduction:

In recent years, $LiNbO_3$ crystals have been extensively used in optical information technologies, such as the holographic storage, optical interconnection, and optical neural network. Several advantages make this crystal attractive. High optical quality $LiNbO_3$ with diameters larger than 2 inches can be grown. Furthermore, the photorefractive characteristics of the crystals can be modified, either by adding doping impurities such as transition metals in the congruent melts or by adjusting appropriate reduction atmosphere during the thermal annealing process. Typically, for photorefractive applications, the iron doped $LiNbO_3$ crystals are cut into a thickness of 1mm to 1cm, and the doping concentrations of iron are in the range of 0.01% to 0.05% mole weight. This thickness and doping concentration provide suitable optical absorption property both for producing photorefractive effect, and at the same time allowing good transmission for optical information. Under moderate optical illumination intensities ($\sim W/cm^2$), the characteristic time for writing a hologram in the $Fe:LiNbO_3$ crystal is in the range of minutes. This characteristic time is very long compared with that of other photorefractive crystals. For example, the typical time constant for BSO is about 10^{-2} sec. However, following the calculation from Yeh [1], it shows that the response time of typical $LiNbO_3$ is far greater than the theoretical limit due to the number of absorbed photons. This suggests that it is possible to increase the response speed of $LiNbO_3$ by adjusting parameters in the process of producing crystals. In 1972, Staebler et al. have demonstrated that the transition metal impurity, especially the Fe could be used to enhance the storage sensitivity [2]. The high recording and erase sensitivities were observed in the heavily reduced samples of the lightly doped $LiNbO_3$ crystal [3].

In this paper, we present a real-time optical image recognition system using a thin $Fe:LiNbO_3$ plates and discuss the preparation of thin plates for real-time optical information processing. We first describe the principles of the photorefractive perceptron learning algorithm. An experiment of the optical neural network for shift-invariant image classification is demonstrated. Then we present our research on the influence of the doping concentration in

photorefractive thin plates on the diffraction efficiency and the response speed of holographic gratings. Both theoretical analysis and optical experiments are described. Our result shows that the impurity doping concentration of $Fe:LiNbO_3$ crystal provides us a method for controlling the temporal characteristic of the thin crystal plates and this provides us a useful guide for designing crystals for various image processing applications.

2. The photorefractive neural network for shift-invariant image recognition

Several types of photorefractive (PR) neural networks have been proposed and demonstrated for the implementation of the perceptron learning algorithm[4-6]. In these systems the interconnection weights of the neural networks are recorded as holographic gratings stored in PR crystals such as $BaTiO_3$ and $LiNbO_3$. In this paper we consider a single layer perceptron network. The network consists of N-input units, a N-dimensional interconnection weight vector w and one output neuron. The network is trained to classify a set of training patterns $\{x_1, x_2, \ldots, x_M\}$ into two classes C1 and C2, depending on whether the value of the inner product $|w \cdot x_n|$ is greater or smaller than the threshold value θ. During the learning stage, the network is trained according to the learning algorithm to find an appropriate w for the desired classification. Finally, the interconnection weight w is used as a matched filter for image correlation.

We first describe the training procedure of the optical perceptron. The updating rule of the photorefractive perceptron can be described by the following expression [7] :

$$w(p+1) = w(p)e^{-|\alpha(p)|t/\tau} + \sigma(p)[1 - e^{-t/\tau}]x(p) \tag{1}$$

where τ is the writing time constant of the crystal. Here, for a simple illustration, we assumed that the writing time and decay time constants are equal. t is the exposure time for each pattern and $x(p)$ is the input pattern at the pth iteration. $w(p)$ is the interconnection weight vector at the pth iteration and the updating signal $\alpha(p)$ is expressed by :

$$\alpha(p) = \begin{cases} 0 & \text{if } x(p) \text{ is correctly classified} \\ 1 & \text{if } x(p) \in C1, \text{ but } |w(p) \cdot x(p)| < \theta \\ -1 & \text{if } x(p) \in C2, \text{ but } |w(p) \cdot x(p)| > \theta \end{cases} \tag{2}$$

where θ is the threshold value for the classification. It has been shown that proper selections of θ as well as the exposure time t are crucial for the learning procedure [7,8]. If the value of θ is set too low then the patterns in the C2 class will be easily misclassified as class C1, and if θ is chosen too high then it is difficult to obtain a correct w for classifying the C1 patterns. In either case, the learning will take a large number of iterations to converge or will never converge. In our research, we use the self inner product of a pattern $x \cdot x$, where x is a training pattern belongs to class C1, as the reference value. θ is taken to be one tenth of this value. On the other hand, we set the exposure time t as one tenth of the time constant of the photorefractive crystal.

Our experimental setup of the photorefractive perceptron is shown in Fig. 1. The detailed principle and experimental design of this system have been described in Refs 9 and 10. Here, we only briefly describe the main procedures of operation. As shown in Fig. 1, a personal computer is used for the control of the learning system. Shutters S1, S2 and S3 and two beam-splitters form a double Mach-Zehnder interferometer for realizing the recording and erasure of the holographic gratings by using the Stoke theorem for wave reflection and transmission. This interferometer provides a phase control of either 0 (with shutters S1, S3 opened and S2 closed) or π (with shutters S2, S3 opened and S1 closed) phase-shift relative to the initial reference interference fringes. By combining these two operations, the learning algorithm of the photorefractive perceptron has been implemented.

During the learning stage, each of the training patterns is sent one by one by the computer to the LCTV as the input to the perceptron. The magnitude of the inner product of the input pattern and the interconnection weights is detected by the photodetector and then compared with the desired value which is stored in the personal computer. Then an error signal is generated and is used by the computer to turn on the appropriate shutters (S3 and S1 or S2) for updating the weights. The learning procedure continues until all the patterns are correctly classified. Then the optical filters stored in the $LiNbO_3$ crystal can be used for image correlation.

In our optical experiment, a LiNbO$_3$ thin plate was used for storing the interconnection weights. The thickness of the LiNbO$_3$ plate is 250 μm. The focal length of L1 is 84.1 cm. This arrangement provides the system with a shift invariant range of 2.5 cm for image correlation experiments. This range is good for almost the whole size of the LCTV screen. Fig. 2 shows the training patterns used in our experiments. Each class is one kind of fish which has faces at opposite directions. Before the learning procedure, we first perform optical image correlation experiment. Two images of the class C1 fish are used to form a composite filter in the crystal by the double exposure technique. Since the plate thickness and lens focal length together satisfy the condition of thin holograms, the system posses the property of shift invariant. The input image for the image correlation experiment comes from a video tape and is displayed on the LCTV. Thus the system performs a shift invariant real-time image recognition. Fig. 3 shows one frame of the output of image correlation. We then perform the learning procedure. After the learning is complete, the interconnection weights recorded in LiNbO$_3$ are also used for image correlation. The new correlation output is shown in Fig. 4. Comparing the Fig. 4 and Fig. 3, it is seen that the cross-correlation that has been produced by class C2 fish was reduced dramatically by the learning procedure.

Note that the range of the shift invariant is dependent on the thickness of the photorefractive thin plate and the focal length of L1. If one wants to setup a compact system with a short focal length, then we need a thinner holographic recording plate. For example, if we used 20 cm focal length and hope to get a shift invariant range of 3cm, then the thickness of the photorefractive plate has to be reduced to 50μm. In the following section, we describe how to design the thin plate which can be used for this purpose.

3. Thin photorefractive crystal plates for real-time image processing

According to the band transport model proposed by Kukhtarev et al.[11], phase gratings can be recorded in a photorefractive medium through the modulation of the refractive index. There are three processes involved : photo-excitation, drift or diffusion, and retrapped. The three processes arise from the charge transport occurred between band traps. The empty traps N_A (acceptor) and the occupied traps N_D (donor) play important roles in determining the photorefractivity of the materials. In words, the incident photons generate photoelectrons from the donor impurities. Then electrons are being transported in the conduction band, recaptured by the ionized impurities, and finally a space charge distribution is created. In Fe:LiNbO$_3$, the Fe^{3+} and the Fe^{2+} play the roles of the N_A and N_D respectively. High doping concentration of the impurity affects the absorption coefficient of the crystal and hence the photorefractivity of the crystal. In general, the diffraction efficiency η of the transmission photorefractive grating can be given by the relation[1]

$$\eta = e^{-\alpha d} \sin^2\left(\frac{\pi d}{2\lambda \cos\theta} n^3 r_{eff} E_{SC}\right) \tag{3}$$

where

$$\alpha = s(N_D - N_D^i)/h\upsilon \tag{4}$$

$$E_{SC} = E_q \frac{iE_d}{E_q + E_d} \frac{I_1}{I_0} \tag{5}$$

with

$$E_d = \frac{k_B TK}{q}$$

$$E_q = \frac{qN_A(N_D - N_A)}{\varepsilon K N_D}$$

where α is the photo absorption coefficient, d is the thickness of the crystal, r_{eff} is the effective electro-optical coefficient that is appropriate for the crystal orientation and incident polarization, E_{SC} is the space charge field, s is the cross section for photoexcitation, N_D^i is the ionized donor impurity, which is almost equal to N_A when the electron density is small, hυ

is the energy of the incident photon, I_1 is the modulation depth of the input light intensity, I_0 is the average light intensity, k_B is the Boltzman constant, T is the temperature, q is the electron charge, ε is the dielectric constant and K is the grating vector. The response time τ of the crystal can be expressed as :

$$\tau = t_0 \frac{E_d + E_\mu}{E_d + E_q} \tag{6}$$

and

$$t_0 = \frac{N_A}{N_D s I_0}$$

$$E_\mu = \frac{\gamma N_A}{\mu K}$$

where γ is the electron-ionized trap recombination rate, μ is the electron mobility, E_μ is the drift field, and t_0 is a characteristic time constant of the medium.

The above equations show the relationships between the diffraction efficiency, the response time of the holographic gratings and the concentration of the donors and the acceptors. It is seen that in Eq. 3, the diffraction efficiency depends on the concentration of the donors and acceptors. Under typical conditions, $N_A \ll N_D$, hence E_q is proportional to N_D. Since $E_d \ll E_q$, thus E_{sc} is proportional to E_q, and it turns out that E_{sc} is proportional to N_D. Therefore, as the concentration N_D increases, the diffraction efficiency increases. On the other hand, optical absorption also increases with the doping concentration. Therefore, when the absorption is too large, the diffraction efficiency will become a decreasing function of the doping concentration. In Eq. 6, t_0 is the important parameter of the response time. It is proportional to N_A/N_D. As the impurity concentration N_D increases, the response time is decreased. Given the parameters in Table 1, we calculated the diffraction efficiency and the time constant for various doping concentrations. The results are plotted in Fig. 5 and Fig. 6.

Fig. 5 shows the relationship of the diffraction efficiency and the donor concentration for $N_A/N_D = 0.1$, 0.05 and 0.01. The figure shows that the diffraction efficiency increases rapidly with the donor concentration, and it has a peak value for some appropriate doping concentration. Then the diffraction efficiency decays when the donor concentration is further increased. It also shows that the peak value of the diffraction efficiency is increased as the ratio N_A/N_D increases.

Fig. 6 plots the variation of the response time τ as a function of the donor concentration for $N_A/N_D = 0.1$, 0.05, and 0.01. The figure shows that the response time decreases with the donor concentration, and it is also decreases when the ratio of N_A/N_D is decreased. This provides us a useful message for designing thin photorefractive plates for real-time image processing applications. In order to obtain a thin plate with fast response, we should keep N_A/N_D as low as possible. However, this will reduce the diffraction efficiency of the plates. Therefore, a compromise has to be made between the two requirements.

Now we describe optical experiments. The crystal samples used in this experiment was a series of crystal plates with different doping concentrations. Firstly, $LiNbO_3$ single crystals with Fe_2O_3 doping concentrations varying from 0.06% to 1.5% mole are grown by using Czochraski technique. Then, it is x-cut and polished to a thickness of about 36μm. Each thin plate is adhered on an optical glass (BK7) with optical adhesive. The structure of the thin plate is shown in Fig. 7. In order to realize the effect of the doping concentration, we measured the optical transmission of these plate in the spectrum range of 400 ~ 600 nm. Our results show that the absorption increases as the doping concentration is increased. A typical curve of the transmission spectrum of a 1.5% mole plate is shown in Fig. 8.

Fig. 9 shows the experimental setup for measuring the response time of the holographic plates. An extra-ordinarily polarized plane wave from an argon laser ($\lambda = 514.5$nm) is split into two beams. The two beams incident symmetrically into the crystal plate with an intersection angle of 3.3 degrees and the grating vector is parallel to the c-axis. The total

incident intensity is about 4 W/cm^2. A weak extra-ordinarily He-Ne laser is incident from the back side of the plate to probe this photorefractive grating. The wavelength of the probe beam is 632.8 nm and the intensity is about 0.1 W/cm^2. We measured the first order diffraction intensity. Fig. 10 shows the temporal behavior of the grating formation and dark decay for a plate with doping concentration of 1.5% mole. It is seen that the build-up time of the grating is about 100 msec and the dark decay time constant is 60 msec. Comparing this with the conventional lightly doped LiNbO$_3$ crystals which have long response time and dark decay time (mins~hours), we see that heavy doping have improved the response speed. By the above analysis, this results in a faster response speed than that of the lightly doped LiNbO$_3$ crystals. We have measured the build-up time for various doping concentrations and the results are shown in Fig. 11. It shows that the response time indeed decreases as the doping concentration increases. When the concentration is increased to 1.5% mole, the response time decreases to about 50 msec and this is close to the fundamental limit calculated by the technique suggested in [1].

In addition, we also measured the diffracted power as a function of the doping concentrations, as shown in Fig. 12. Under our experimental conditions, it is observed that the maximum diffraction efficiency was obtained when the doping concentration is equal to 0.1% mole. From Fig. 11, we know that the response time for this crystal is about 10 seconds. When the doping concentration is increased, the absorption increases and the diffracted light through the crystal is decreased. But in the contrast the response time is decreased. Thus, a trade-off between the diffraction efficiency and the response time has to be considered when we design a photorefractive crystal for real-time image processing applications. This is again in agreement with our theoretical analysis.

4. Conclusion

In this paper, we have demonstrated a real-time and shift-invariant image recognition using photorefractive crystal plates. This system combines the advantages of the learning capability of the perceptron network and the parallel processing of optical systems. Then, we discussed the temporal behavior of the heavily doped Fe:LiNbO$_3$ crystals, both theoretically and experimentally. We have shown that by adjusting the dopant concentrations of Fe$_2$O$_3$, the diffraction efficiency and the response time of the crystals can be controlled. Our results show that heavily doped crystals provide fast response time. They are suitable for real-time optical processing. On the other hand, lightly doped crystals produces higher diffraction efficiency and longer response time. They are suitable for applications such as optical information storage.

Acknowledgment

References

1. P. Yeh, " Introduction to photorefractive nonlinear optics ", pp.105, (Wiley, New York, 1993).
2. J. J. Amodei, W. Phillips and D. L. Staebler, "Improved electro-optic materials and fixing techniques for holographic recording", Appl. Opt. 11, 390-396(1972).
3. D. L. Staebler, W. J. Burke, W, Phillips, and J. J. Amodei, "Multiple storage and erasure of fixed holograms in Fe-doped LiNbO$_3$", Appl. Phys. Lett. 26, 182-184 (1975).
4. J. J. Hopfield, " Neurons networks and physical systems with emergent collective computational abilities", Proc. Natl. Acad. Sci. U.S.A.,79, pp. 2554-2558 (1982).
5. J. J.Hopfield, " Neurons with graded response have collective computational properties lide those of two-state neurons", Proc. Natl. Acad. Sci. U.S.A., 81, pp.3088-3092 (1984).
6. K. Y. Hsu, H. Y. Li, D. Psaltis, " Optical implementation of a fully connected neural network", Proc. IEEE, 78, pp.1637-1645 (1990).
7. K. Y. Hsu, S. H. Lin & P. Yeh, " Conditional convergence of photorefractive perceptron learning", Opt. Lett., 18, pp. 2135-2137 (1993).
8. K. Y. Hsu, S. H. Lin & T. C. Hsieh, " A hybrid Neural Network for Image Classification", Opt. and Laser. in Eng. 23, pp.167-183 (1995).

232

9. J. Hong, Campbell, S. & P. Yeh, " Optical pattern classifier with perceptron learning", *Appl. Opt.*, 29, pp.3019-3025, 1990.
10. K. Y. Hsu, S. H. Lin, C. J. Cheng, T. C. Hsieh & P. Yeh, "An optical neural network for pattern recognition", *Int. J. Opt. Comput.*, 2, pp.409-423,1991.
11. N. V. Kukhtarev, " Kinetics of hologram Recording and Erasure in Electro-Optic Crystals", Sov. Tech. Phys. Lett., 2, No. 2, pp.438 (1976).
12. M. Carrascosa and F. Agullo-Lopez, " Theoretical modeling of the fixing and developing of holographic gratings in LiNbO$_3$", J. Opt. Soc. Am. B, Vol. 7, No. 12, pp. 2317-2322 (1990).

Symbol	meanings	value
d	the thickness of the crystal	50 μm
θ	the incident angle	2°
I_1/I_0	the modulation depth	0.001
γ	the electron-ionized trap recombination rate	$1*10^{-15}$
μ	the electron mobility	0.8 cm^2/(V*sec)
s	the cross section for photoexcitation	10^5 cm^2/J
λ	the input wavelength	514.5 nm
T	temperature	300 K
k_B	Boltzman constant	$1.38*10^{-23}$ J/K

Table 1 The parameters for LiNbO$_3$.[1,12]
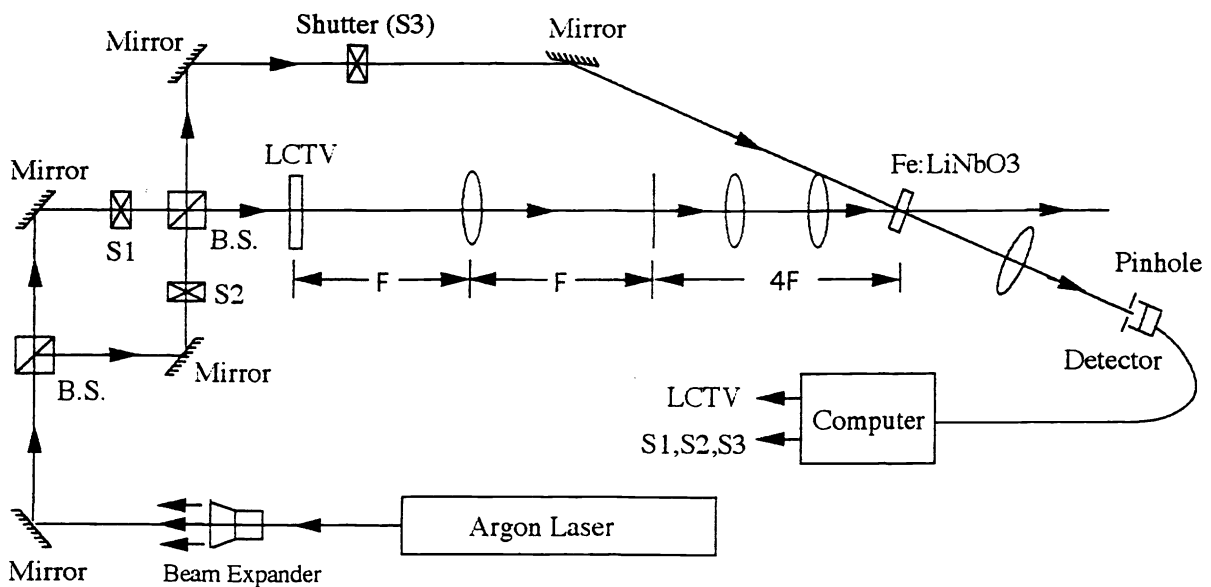
Figure 1 The experimental setup of the optical image recognition system

233

	Image	
C1		
C2		

Figure 2 The training images
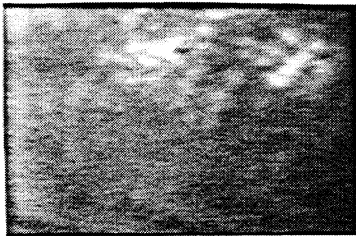
Input image	Correlation output

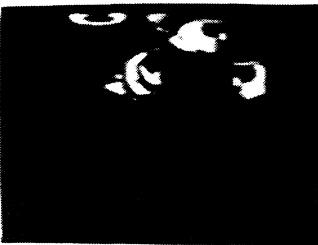Figure 3 The correlation output before training

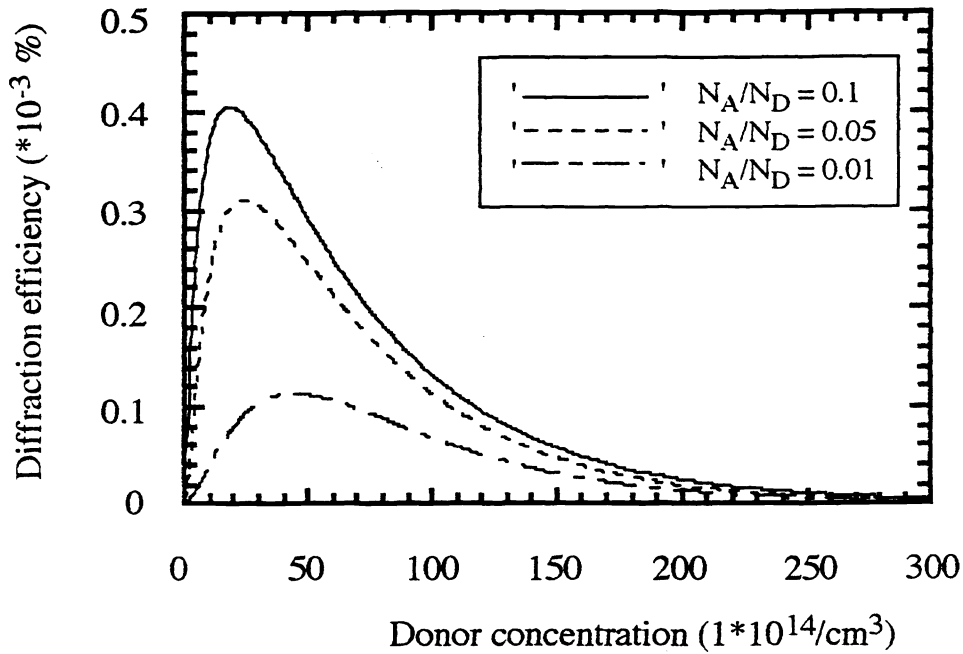| Input image	Correlation output

Figure 4 The correlation output after training

234

Figure 5 The function of the diffraction efficiency as the donor concentration
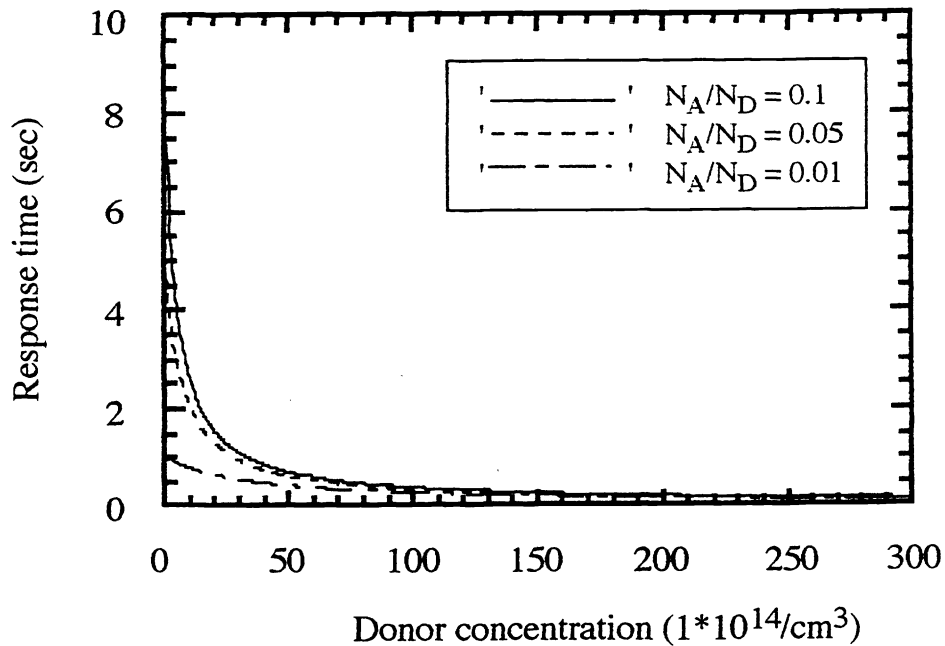for $N_A/N_D = 0.1$, 0.05 and 0.01

Figure 6 The function of the response time as the donor concentration
for $N_A/N_D = 0.1$, 0.05 and 0.01

235
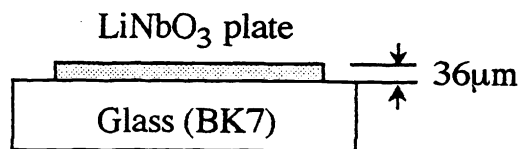
Figure 7 The structure of the LiNbO$_3$ thin plate
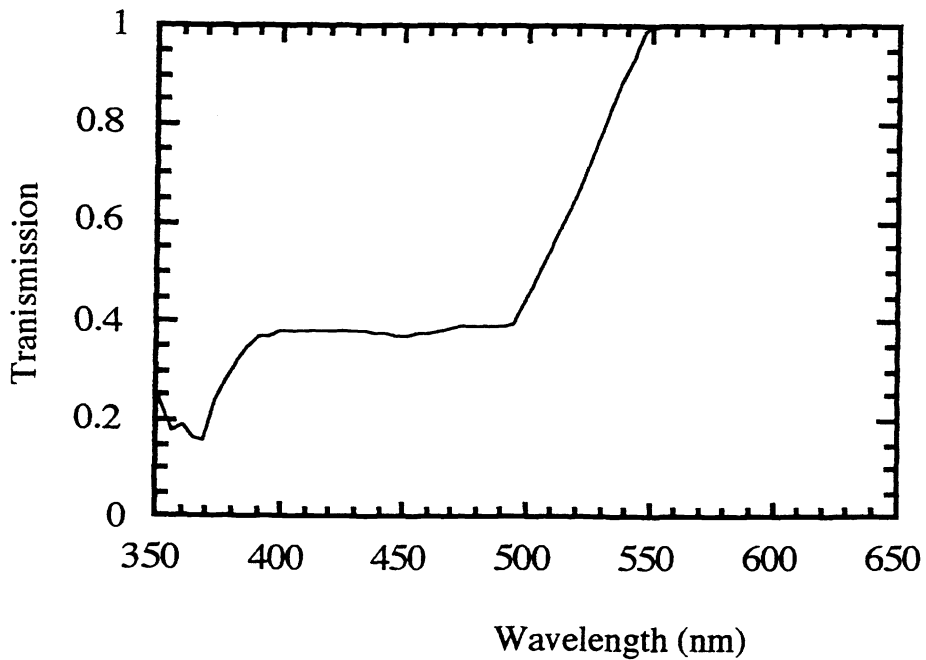
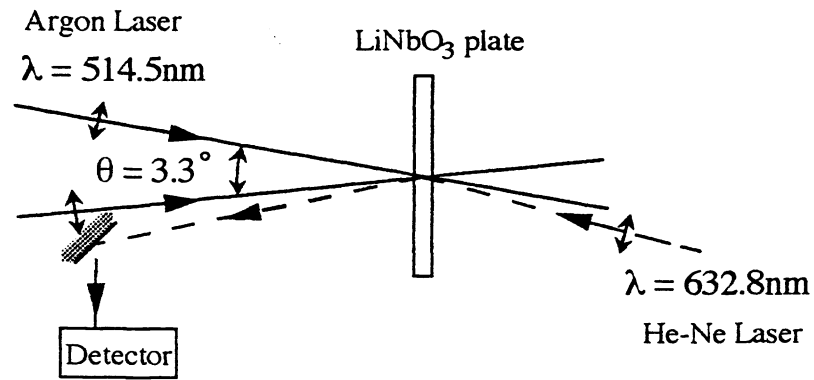Figure 8 The trainsmission spectrum of the 1.5% mole Fe : LiNbO3

Argon Laser
λ = 514.5nm

LiNbO₃ plate

θ = 3.3°

Detector

λ = 632.8nm
He-Ne Laser

Figure 9 The experimental setup for photorefractive grating
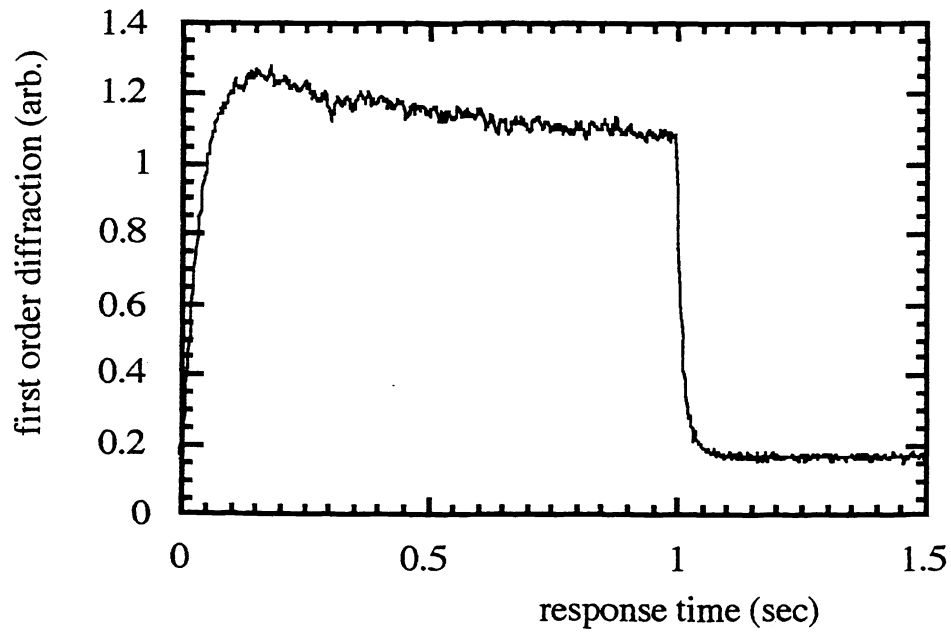
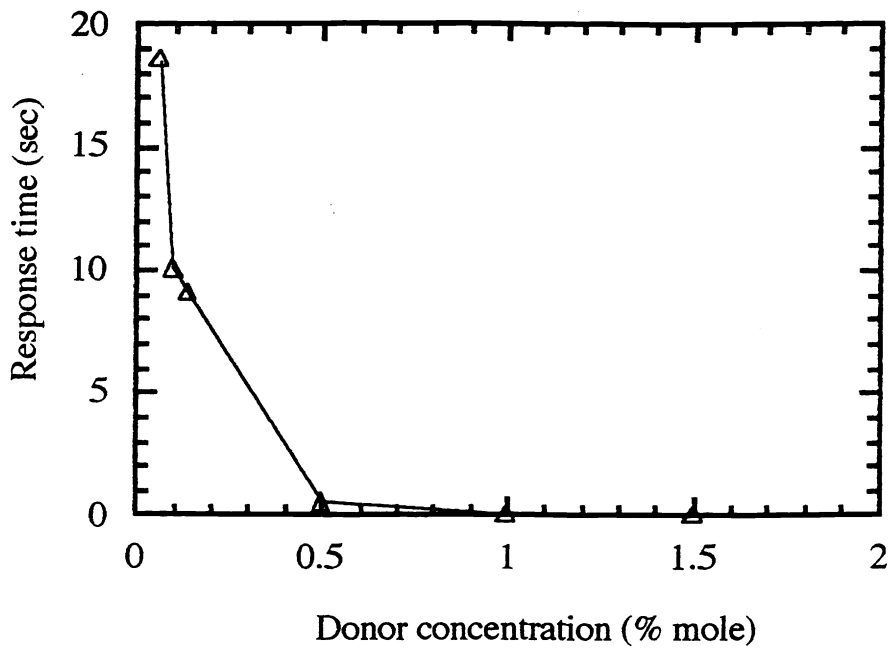Figure 10 The grating response time of the 1.5% mole Fe : LiNbO3

237

Figure 11 The response time vs the donor concentration. (experimental results)
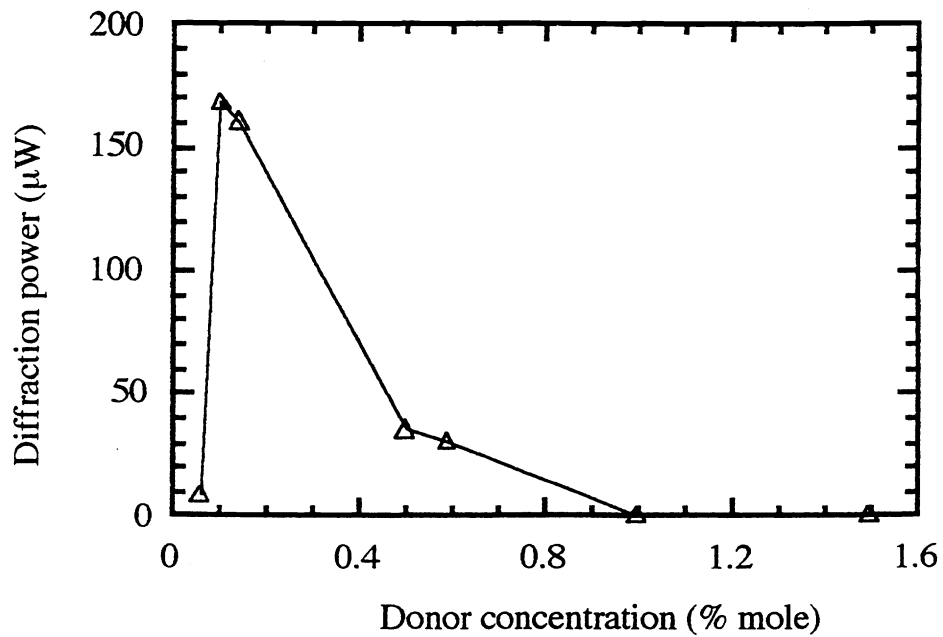
Figure 12 The diffraction efficiency vs the donor concentration (experimental results)

238